



PAPER • OPEN ACCESS

Ionic liquid coated zerovalent manganese nanoparticles with stabilized and enhanced peroxidase-like catalytic activity for colorimetric detection of hydrogen peroxide

To cite this article: Sajid Rauf *et al* 2020 *Mater. Res. Express* **7** 035018

View the [article online](#) for updates and enhancements.

You may also like

- [Bandgap control of -Fe₂O₃ nanozymes and their superior visible light promoted peroxidase-like catalytic activity](#)
Mingyun Zhu, Yunqian Dai, Yanan Wu et al.
- [Platinum group element-based nanozymes for biomedical applications: an overview](#)
Shao-Bin He, Liu Yang, Meng-Ting Lin et al.
- [Lamellar shape lead tungstate \(PbWO₄\) nanostructures as synergistic catalyst for peroxidase mimetic activity](#)
Naveed Akhtar Shad, Muhammad Munir Sajid, Yasir Javed et al.

Breath Biopsy Conference



5th & 6th November
Online

BREATH
BIOPSY



Join the conference to explore the **latest challenges** and advances in **breath research**, you could even **present your latest work!**

Register now for free!



Main talks

Early career sessions

Posters

Materials Research Express



PAPER

Ionic liquid coated zerovalent manganese nanoparticles with stabilized and enhanced peroxidase-like catalytic activity for colorimetric detection of hydrogen peroxide

OPEN ACCESS

RECEIVED
18 January 2020

REVISED
4 March 2020

ACCEPTED FOR PUBLICATION
11 March 2020

PUBLISHED
23 March 2020

Original content from this work may be used under the terms of the [Creative Commons Attribution 4.0 licence](#).

Any further distribution of this work must maintain attribution to the author(s) and the title of the work, journal citation and DOI.



Sajid Rauf¹ , Nasir Ali² , Zuhra Tayyab¹, MAK Yousaf Shah⁷ , Chang Ping Yang^{1,8}, JF Hu³, Weiguang Kong⁵, QA Huang⁶, Akhtar Hayat^{4,8} and Nawshad Muhammad⁴

- ¹ Hubei Collaborative innovation center for advanced Organic Chemical Materials, Faculty of Physics and Electronic Science, Hubei University, Wuhan, Hubei 430062 People's Republic of China
- ² Zhejiang Province Key Laboratory of Quantum Technology and Devices and Department of Physics, State Key Laboratory for Silicon Materials, Zhejiang University, Hangzhou, 310027, People's Republic of China
- ³ Faculty of Materials Science and Engineering, Taiyuan University of Science and Technology, Taiyuan, 030024, People's Republic of China
- ⁴ Interdisciplinary Research Centre in Biomedical Materials (IRCBM) COMSATS University Islamabad, Lahore Campus 54000, Pakistan
- ⁵ Hebei Key Laboratory of Optic-electronic Information and Materials and National-Local Joint Engineering Laboratory of New Energy Photoelectric Devices, College of Physics Science and Technology, Hebei University, Baoding 071002, People's Republic of China
- ⁶ College of Science/Institute for Sustainable Energy, Shanghai University, Shanghai 200444, People's Republic of China.
- ⁷ Engineering Research Center of Nano-Geo Materials of Ministry of Education, Department of Materials Science and Chemistry, China University of Geosciences, 388 Lumo Road, Wuhan, 430074, People's Republic of China
- ⁸ Authors to whom any correspondence should be addressed.

E-mail: cpyang@hubu.edu.cn and akhtarhayat@cuilahore.edu.pk

Keywords: zero-valent manganese nanoparticles, modulator and stabilizer ionic liquid, ionic liquid coated nanoparticles, optical detection, hydrogen peroxide.

Supplementary material for this article is available [online](#)

Abstract

Nanomaterials based colorimetric detection is an area of vital importance in the field of sensing applications. The nanoparticles are the main component of colorimetric sensor in replacing the natural enzyme based sensor. In this context, zero valent nanoparticles have revolutionized the field of optical sensing especially due to easily shift of electron, facile and low cost of preparation, and ease of surface modification. In this work, zero valent manganese nanoparticles (ZV-Mn NPs) are prepared through a simple and very quick method and modulated with new type of ionic liquid (IL). As-prepared materials were characterized through FE-SEM, HR-TEM, BET, FTIR, and XRD. Subsequently, the peroxidase like catalytic activity of pure and modified ZV-Mn NPs to catalyze oxidation of N,N',N,N'-tetramethylbenzidine (TMB) in the presence of hydrogen peroxide (H₂O₂) investigated. Moreover, the absorbance peak is observed at wavelength 652 nm. The enhanced catalytic activity of ZV-Mn NPs was attributed to the fast transfer of electron mechanism in between substrate and H₂O₂. The coating of IL on ZV-Mn NPs permitted a low limit of detection 0.2 μM with a linear range of 10–280 μM. This work can find wide spread interest in the colorimetric sensing applications. In order to verify the successful demonstration of H₂O₂ sensor, we have applied it in the dairy milk products with satisfactory results.

1. Introduction

Hydrogen peroxide (H₂O₂) is one of the important constituents of the human body, which is formed as a by-product of oxidative metabolism in the organism. A large number of oxidases through catalytic reaction produces H₂O₂. There is a key role of naturally existing peroxidase in the biological system for the catalytic degradation of H₂O₂ [1]. The concentration of hydrogen peroxide is regulated by peroxidase, which is normally produced by the kidneys and red blood cell of the human body [2]. In this sequence, the concentration of

hydrogen peroxide is controlled by the peroxidase, but the favorable working conditions are required (e.g., temperature, pH, and time, etc) [3]. Hydrogen peroxide is considered to be a significant mediator in food, clinical, industrial, pharmaceutical, and environmental analyses [4]. Many analytical techniques were widely utilized for the detection of hydrogen peroxide such as electrochemical [5–14], titrimetry [15], fluorescence [16, 17], and colorimetric [18–26]. In comparison with other reported methods, there are considerable advantages of colorimetric detection of various analytes over other conventional sensing techniques e.g., cost-effectiveness, facile and reliable method, and practicability and quick response. The visualization of the color variations to the unaided eye during the course of the reaction is the most attractive characteristic of colorimetric sensing. Subsequently, there exist two different routes of colorimetric detection of hydrogen peroxide based on enzyme and nanomaterials [20]. Detection based on nanomaterials has been considered to be more suitable than natural enzymes. Natural enzymes have high selectivity and specificity to the substrates; however, some drawbacks are associated with enzymes, such as high cost, instability, denaturing phenomenon, gentle handling, and required controlled environment [27].

Since in the past two decades, natural enzymes were replaced with artificial nano-enzymes having the remarkable advantages like, easy preparation, cost-effectiveness, large surface area, high catalytic activity, stability, and comfort in manipulation as compared to natural enzymes [28]. This is all possible just because of the integration of nanotechnology to substitute natural enzymes containing many bottlenecks [29]. In this context, large number of nanoparticles (NPs), including magnetic NPs, noble metals NPs, metal oxide NPs, polyoxometalates, conjugated polymers, and carbon materials as well as their derivatives have been employed as a nanozymes to displace the natural enzymes [30–33]. However, artificially designed biomimetic NPs mainly suffer from poor dispersion, low catalytic activity, less surface area, and precipitation under harsh atmospheric conditions. Therefore, it is inevitably needed to search for new approaches to prepare the low-cost biomimetic NPs to overcome the above limitations of nanozymes. The combination of ionic liquids (ILs) and nanoparticles can be employed to obtain high dispersibility, simple procedure of preparation, large surface area, and high as well stable catalytic activity under various pH and different temperatures [29, 34].

Ionic Liquids (ILs) prepared by the combination of fused salts and maintained the low melting point below 100 °C are the fascinating characteristics of organic solvents in the field of chemistry. ILs have been recognized as an organic solvent having negligible vapor potential, wide temperature range, high stability, and tune-able properties with suitable functionalization of cations and anions, as well the capability of dispersing numbers of materials [35]. These versatile characteristics of ILs have been used in a variety of applications [36, 37]. Furthermore, in order to enhance the catalytic performance of catalyst various literature have been reported that ILs have the properties to enhance the catalytic performance and stabilize the reactive catalytic species or reaction intermediates [38]. More significantly, ILs have been used as a modulator in artificial enzymes as well as stabilizing mediator to thermally stabilize the enzymatic product, consequently make it possible to occur the catalytic reactions at high temperature [39].

In this work, all of these unique features are integrated to design a novel construct of nanoparticles modified with an ionic liquid to synergistically enhance the stability and detection limits of colorimetric sensors. Zerovalent Manganese (Mn) nanoparticles (ZV- Mn) NPs were used as promising peroxidase mimics for colorimetric detection of H₂O₂. Mn NPs were prepared by a quick, low cost, and facile method and characterized with various characterization tools, such as FE-SEM, HR-TEM, BET, FTIR, and XRD. The as-prepared ZV-Mn NPs were modified with a new type of IL i.e. 1-H-3-Methylimidazolium formate (HMIM OF) to enhance the catalytic activity, high thermal stability, and high dispersibility as compared to other peroxidase mimetics for colorimetric detection of H₂O₂.

2. Materials and methods

2.1. Reagents and materials

All the chemicals including Manganese (II) chloride (MnCl₂·4H₂O, 99%), N,N,N,N-tetramethylbenzidine (TMB), L-Ascorbic acid, Dimethyl sulfoxide (DMSO) and sodium borohydride (NaBH₄) were purchased received from Sigma Aldrich (<https://www.sigmaaldrich.com/>). Hydrogen peroxide (H₂O₂, 35%) was obtained from MerckGaA (<https://www.merckgroup.com/en>). 1-methylimidazole C₄H₆N₂ (99.2%) and Phosphate buffer saline (PBS, pH=7.4) were acquired from Alfa Aesar (<https://www.alfa.com/en/>). Dopamine was obtained from MerckKGaA (<https://www.merckgroup.com/en>). Formic acid CH₂O₂ (98%–100%) was received from BioM. Urea (98%) was obtained from ACROS (<http://www.acros.com/>). Cuvettes (Quartz) of 10 mM were purchased from Hangzhou CHN Spec Tech. having a capacity volume of 2 ml. The most important thing is that all chemicals used were of without further purifications. All the solutions were made in deionized water from ELGA PURELAB® Ultra water deionizer.

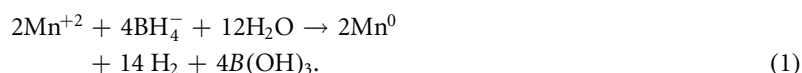
2.2. Characterization

Double beam Perkin Elmer UV–vis spectrophotometer Lambda-25 (UV-25, Perkin Singapore) was utilized to record the UV–vis absorption spectra in a 10 mm disposable cuvettes capacity of containing solution 2 ml and 1 nm bandwidth setting in the range of 400–800 nm.

Field Emission Surface morphology of ZV-Mn NPs was studied using the Field emission scanning electron microscope (FESEM, JEOL JSM7100F Japan). Accelerated voltage of 10 kV applied to take images at alter magnification. The internal structure, the shape of the material and the elemental distribution of as prepared Mn NPs were studied through a Tecnai G2 F30 S-TWIN 300 kV / FEG High resolution transmission Electron Microscopy (HR-TEM) of the as-prepared materials equipped with the BRUKER energy dispersive spectrometer (EDS). The surface area, pore volume, pore size and adsorption and desorption of Nitrogen gas of ZV-Mn NPs were measured through surface area and porosity analyzer Brunauer–Emmett–Teller (BET; Mike Tristar II 3020 Version 3.02, USA) of Micrometrics Instrument Corporation. The functional groups attached to ZV-Mn NPs were studied through Fourier-transform Infrared (FTIR) spectra using Thermo Fisher Scientific (Nicolet iS 50) spectrometer over the wave range of 400–4000 cm^{-1} at a resolution of 8 cm^{-1} . The crystal structures of ZV-Mn NPs were investigated using as-prepared powder by Bruker D8 advanced X-ray diffractometer (Germany, Bruker Corporation with $\text{Cu K}\alpha$ radiation, $\lambda = 1.5418 \text{ \AA}$) over the 2θ range of 20° – 80° with a step of 0.02 degree. All refinement of the XRD was done by MJAD 6.5 software.

2.3. Synthesis of Manganese nanoparticles

Sodium borohydride (NaBH_4 , 140 mM) solution was prepared separately in the deionized deoxygenated water used to avoid any oxidation. At the same time, the manganese Chloride ($\text{MnCl}_2 \cdot 4\text{H}_2\text{O}$, 20 mM) was prepared in a solution of 3 mL ethanol absolute and 22 mL deionized water. The solution of sodium borohydride was added dropwise into manganese chloride solution through titration followed by the simultaneous formation of particles of Mn NPs having black color. During titration, the resulting black materials were stirred for the formation of homogeneity. The proposed reaction for this process is given as follows;



An excess amount of borohydride solution was used for the better formation of ZV-Mn NPs. However, the nanoscale zerovalent manganese (ZV-Mn) was allowed to be aged overnight. After aging, the prepared ZV-Mn was separated by filtration apparatus and micron filter paper ($0.45 \mu\text{M}$) was used to separate solution. To remove the surface impurities attached with particles, the current particles were washed through deionized (DI) water three times and then same with anhydrous ethanol and dried in Oven at 100°C for overnight. After drying, the dried particles were calcined in the furnace at 500°C for 5 h. at the ramp of $5^\circ\text{C}/\text{min}$ followed by ground to get homogenous powder of ZV-Mn NPs. Repeated the same calcination in order to eradicate any possibility of impurity in powder. It was observed that the prepared materials oxidized quickly in the air. Beside other characterizations, the prepared materials were utilized for the sensing applications.

2.4. Preparation of ionic liquid

The 1-H-3-Methylimidazolium formate was prepared using the modified protocol reported by Petrović *et al* [40]. 1-methylimidazole (0.01 mol) was neutralized with formic acid (0.01 mol) in two neck flasks under the cooling condition and subsequently, the resulting mixture was stirred at room temperature for 12 hr to obtain the desired IL medium. Furthermore, to avoid the presence of the unreacted reactants in the solution, the solution was led to the rotary evaporator for 8 hr at 90°C under the moist environment at low pressure. The prepared ionic liquid (after subjecting to rotary evaporator) was characterized using NMR Bruker Avance (500 MHz).

2.5. Coating of nanoparticles

IL coated Mn NPs were prepared in such a way: initially, ZV-Mn NPs (5 mg) was added into the protic IL 1-H-3-Methylimidazolium formate (HMIM OF) (1 mL) and mechanically ground for 30 min in the pestle-mortal until a well-dispersed ionic liquid coated ZV-Mn NPs was achieved. Then prepared dispersed solution was further used for characterizations and colorimetric applications.

2.6. Peroxidase like-catalytic activity of ionic liquid coated nanoparticles

The peroxidase-like activity was evaluated through colorimetric detection of H_2O_2 using N,N,N,N-tetramethylbenzidine (TMB) as a chromogenic substrate. The procedure was carried out as follow; 35 μL of stock solution of dispersed IL coated NPs, 100 μL of TMB (10 mM), 100 μL of Ionic Liquid and 575 μL of phosphate buffered saline were mixed. Subsequently, to investigate the optical change, 100 μL of H_2O_2 (2.8 mM) was added into the reaction solution and was incubated for 5 min as a result a dark blue color was observed.

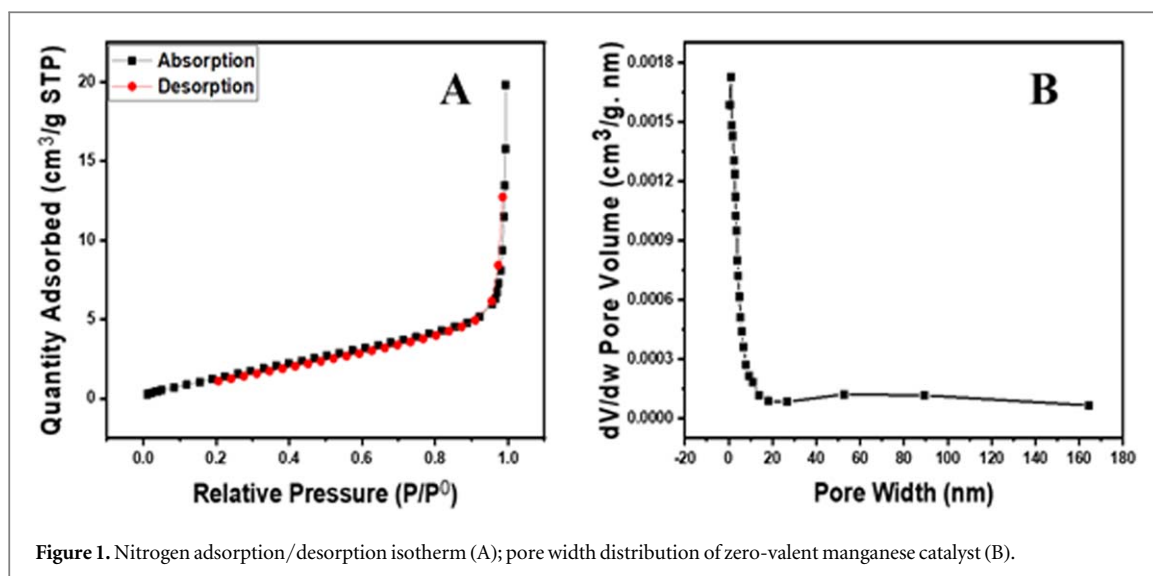


Figure 1. Nitrogen adsorption/desorption isotherm (A); pore width distribution of zero-valent manganese catalyst (B).

Furthermore, UV–vis spectroscopy measurement was used to understand and measure the quantitative relation among IL coated NPs, TMB and varying concentration of H₂O₂ of the resultant solution.

2.7. Detection of Hydrogen peroxide

The detection of hydrogen peroxide was carried out in a similar to the above description but only difference was adding different concentrations of H₂O₂ were mixed in ascending order in total volume of prepared solution very properly. The total solution was incubated for 5 mint at different temperature in the physiological environment, and then the resulting solution was diluted with water for the absorption spectroscopy measurements.

3. Results and discussion

3.1. Characterizations analysis

The inset in figure S1(a) is available online at stacks.iop.org/MRX/7/035018/mmedia presents surface morphology of the ZV-Mn NPs powders. In the image of scanning electron microscopy (SEM) all the particles were distributed homogeneously, which is helpful in generating high area for catalytic activity. High resolution transmission electron microscopy (HR-TEM) images indicated that the particle size of ZV-Mn NPs was less than 50 nm and are well dispersed figure S1(b-c). The small size of ZV-Mn NPs provide a greater surface to volume ratio of the material and thus is responsible for high reactivity due to the greater number of active sites of the reaction. This can be associated with an intense homogeneous nucleation kinetics, where a large number of nucleation sites are formed, mainly due to the molar excess of borohydride added to the manganese salt solution that helped in providing the rapid reduction of the metallic ions; thus, without having time to form nanoparticle clusters, as a result the particle size is nanometric size. The planes provided by x-ray diffraction were verified by the TEM image in figure S1(d). The energy dispersive x-rays analyses were also carried out for ZV-Mn NPs to confirm the presence of the targeted elements at the nano-level with the BRUKER supported energy dispersive x-rays analyses associated with TEM. The elemental mapping is shown in figure S1(e-h). It can be clearly identified that all elements of ZV-Mn NPs are presented in the results confirming the proper synthesis of the proposed ZV-Mn NPs. Moreover, in-line with SEM results, the crystallinity, and homogeneity in the size distribution of particles are confirmed by the XRD analysis where sharp peaks corresponding to reflection from planes are observed.

For pores size distribution and surface area analysis of fabricated zero-valent manganese catalyst, nitrogen adsorption-desorption measurements were used, which is shown in figure 1(A-B). From figure 1(A), it's quite obvious that it belongs to type IV isotherm, which confirms an excellent interaction between adsorbate and adsorbent [41]. The pores sizes were found to be bigger than the molecular diameter of N₂ (3.5 Å), which can be detected by nitrogen adsorption-desorption experiment [42]. In our case, the pore volume was in the range of 10–100 nm, which confirms the mesoporosity of the material [43] see figure 1(B). The specific surface area, pore volume, and pore size were found to be 6.0568 m² g⁻¹, 0.018187 cm³ g⁻¹, and 12.011 nm respectively. The H₂O₂ can be easily absorbed on the fabricated catalyst due to its large surface area that increases the effectiveness of the

reaction. Moreover, it was revealed by the BET results that fabricated catalyst can be used easily for H₂O₂ and other organic pollutants sensing due to its large surface area.

Fourier transform Infrared (FTIR) was performed in order to get information and identify the attached functional groups with ZV-Mn NPs in the range of 500–4000 cm⁻¹, as shown in figure S2. Many peaks were observed in the spectra of manganese nanoparticles such as, at 632.54 cm⁻¹ ascribed to O-Br stretching because the preparation involved the borohydride and partially oxygen got attached. Additionally, a peak observed at 1010 cm⁻¹ that can be assigned to the stretching vibration of O-H hydroxyl group bending belongs to physisorbed water molecules present on the surface of the adsorbent. Likewise, two more strong peaks at 1351 cm⁻¹ and 1604 cm⁻¹ were observed, which can be attributed to the bending vibrations of a hydroxyl group to the metal oxides such M-OH (M = Mn) [44, 45].

In order to get the structural information of ZV-Mn NPs at room temperature, X-ray diffraction analysis was performed as depicted in figure S3. There amorphous peaks of MnO₂ were observed at 23.18°, 53.48°, 67.98°, and 72.32°, which are perfectly matched by JADE 6.5 software. Furthermore, strong peaks were observed for Mn₂O₃ at the 2θ values 18.41°, 29.67°, 35.53°, 61.41°, 66.33° and 73.54° (JCPDS No. 98-006-1726). In addition, the peaks obtained at 32.58°, 43.33°, 44.28°, 48.85°, 58.31°, and 75.11° corresponds to the diffraction peaks of Mn⁰ (JCPDS No. 01-081-7623). However, the major characteristics peaks of Mn⁰ located at 2θ = 40.09° and 41.48° were of very low intensity compared to the characteristic peaks due to the effect of MnO₂ and Mn₂O₃. These results showed that the as-synthesized materials have enough presence of nZV-Mn; as presented in figure S3. It has been reported that the oxidation of Mn to MnO₂ and Mn₂O₃ nanocrystal can take time but it also depends upon environmental conditions and size of particles [46]. From this study, considering the peak at degrees, average particle size has been estimated by using Debye-Scherrer formula;

$$D = \frac{k\lambda}{\omega \cos \theta} \quad (2)$$

Where k and λ are the shape factor (~0.90) and the wavelength of the x-ray (1.5405 Å), respectively. Whereas, ω represents the full width at half-maximum (FWHM) of specified peak and θ is the diffraction angle and D is particle diameter size. The calculated mean crystallite size of the ZV-Mn NPs was approximately 25 nm.

3.2. Peroxidase like activity of Ionic Liquid coated nanoparticles

The peroxidase-like activity of nanoparticles has been investigated by the catalytic oxidation of TMB substrate in the presence of H₂O₂, along with IL as a stabilizing and modulating to enhance the biomimetic activity of a single assay [17, 22, 27]. IL has been widely utilized in the field of biomedical applications. Many methods have been reported to stabilize the nanoparticles and enhance the catalytic activity but coated moieties block the diffusion of other molecules through the surface. Subsequently, the idea was followed to determine the stability of IL, as-prepared nano-zerovalent manganese nanoparticles were dissolved in phosphate buffered saline in the presence and absence of an appropriate proportion of IL. Figure 2(C) shows that IL has displayed a highly dispersive media and enhanced the dispersibility of ZV-Mn NPs for a longer time while on the other side agglomerates/precipitates were formed. IL can stabilize the nanoparticles and can be the possible reason to the formation of ionic layer on the surface of the metal nanoparticles as well as to the enhancement of the catalytic activity. Furthermore, the peroxidase-like catalytic activity of IL coated ZV-Mn NPs was investigated. The catalytic activity of IL coated ZV-Mn NPs was found to be many folds higher than pure ZV-Mn NPs and the intense blue color product was observed in the IL coated ZV-Mn NPs system than that of pure ZV-Mn NPs system under the same experimental conditions, as depicted in the inset of figure 2(A-B). The catalytic activity can be attributed to the metal centers. The peroxidase substrate adsorbed on the surface of IL coated ZV-Mn NPs as a result formation of π-π interaction occurred. However, the interaction of H₂O₂ with metal ions in the presence of molecular oxygen and their conversion to double ●OH helped in the catalytic activity as well as in the oxidation of TMB.

The ZV-Mn NPs easily oxidize in air, get redox state Mn⁺¹, and yield the product of H₂O₂ in the aqueous solution following the Fenton type of oxidation mechanism, the same Fenton type reaction was employed on zero-valent iron nanoparticles as well in iron-copper nanoparticles [47, 48].

The redox reaction can be expressed as following equation;



In addition, hydrogen peroxide easily oxidize the ZV-Mn NPs



It is well known that ZV-Mn NPs are very unstable and can be easily be oxidized into Mn⁺² state and helps in releasing the electron to reduce the other components,

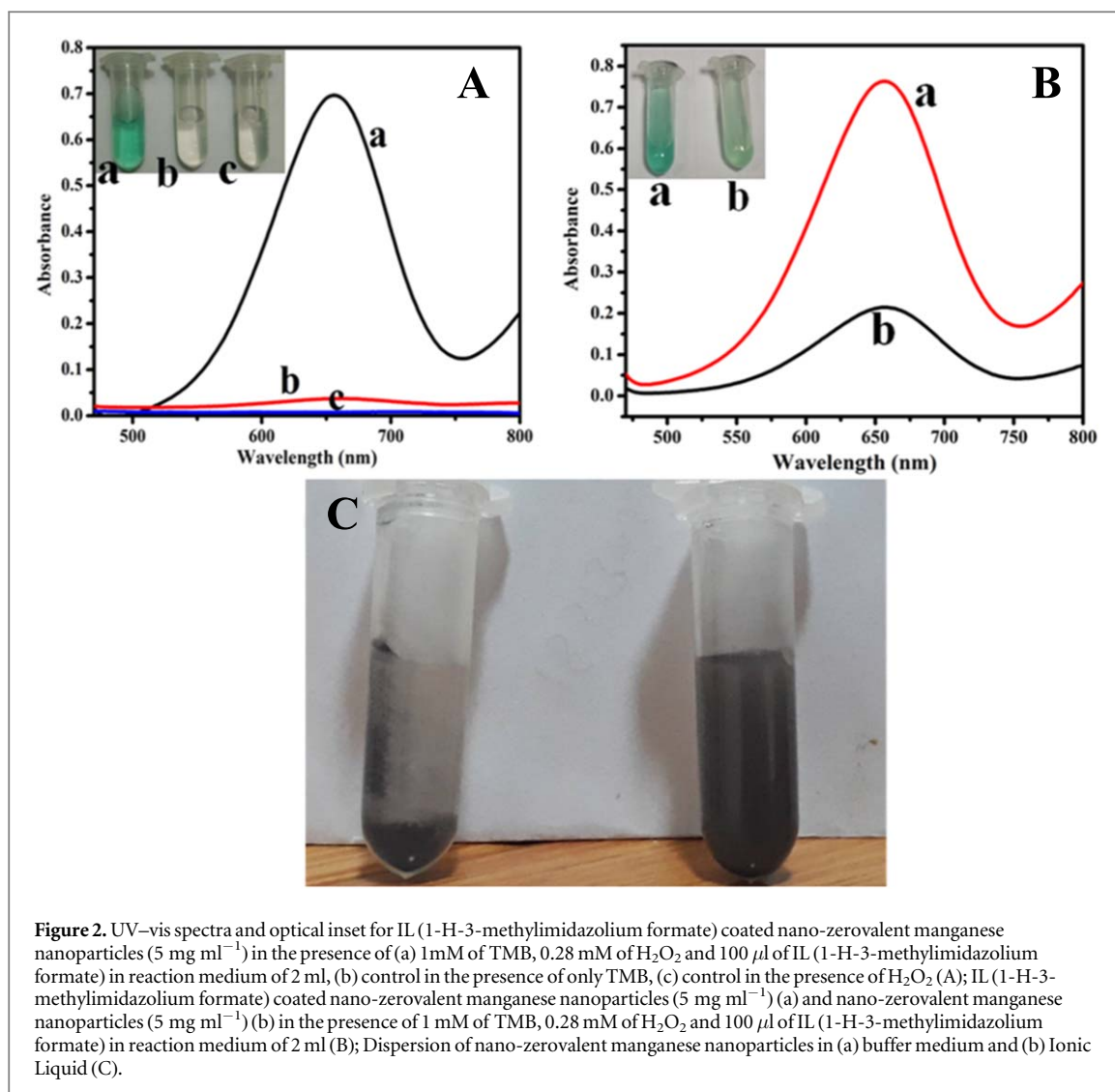


Figure 2. UV-vis spectra and optical inset for IL (1-H-3-methylimidazolium formate) coated nano-zerovalent manganese nanoparticles (5 mg ml^{-1}) in the presence of (a) 1 mM of TMB, 0.28 mM of H_2O_2 and $100 \mu\text{l}$ of IL (1-H-3-methylimidazolium formate) in reaction medium of 2 ml, (b) control in the presence of only TMB, (c) control in the presence of H_2O_2 (A); IL (1-H-3-methylimidazolium formate) coated nano-zerovalent manganese nanoparticles (5 mg ml^{-1}) (a) and nano-zerovalent manganese nanoparticles (5 mg ml^{-1}) (b) in the presence of 1 mM of TMB, 0.28 mM of H_2O_2 and $100 \mu\text{l}$ of IL (1-H-3-methylimidazolium formate) in reaction medium of 2 ml (B); Dispersion of nano-zerovalent manganese nanoparticles in (a) buffer medium and (b) Ionic Liquid (C).



Hence, it is observed from the above chemical reactions that higher oxidation states i.e. $\text{Mn}^{+1}/\text{Mn}^{+2}$ play a key role in the peroxidase catalytic activity of manganese nanoparticles. Furthermore, H_2O_2 adsorbs on the surface of manganese nanoparticles and produces the Mn^{+1} to generate the hydroxyl $\bullet\text{OH}$, the $\bullet\text{OH}$ further help in the oxidation of TMB substrate to generate an intense blue color.

In addition, control experiment was performed where the absorbance of pure ZV-Mn NPs was found to be negligible as compared to IL coated ZV-Mn NPs, as shown in figure 2(A-B). The coating of IL over the manganese nanoparticles played a vital role in the enhancement of catalytic activity. The presence of pi-electron density in both of the imidazolium cations and carboxylate anions in IL were employed to enhance the medium conductivity. The high solvation power of IL is considered to play a positive role in the enhanced catalysis process [30] as well the presence of large number of cations and anions and their weak interactions with oxidized products were further expected to improve the activity. The chemical structure of IL (1-H-3-methylimidazolium formate) is presented in figure S4. Likewise, the decomposition of H_2O_2 into OH radical that is used for further catalyze the oxidation of chromogenic substrate TMB can be associated with the presence of nascent acidic hydrogen of the cationic part of IL.

Interestingly, the color of a catalyzed product was stable for more than 25 h.; afterwards, a slight color loss was observed as compared to the oxidized product in pure buffer medium without IL (maximum degradation occurred approximately after 1 h.) and the relative degradation of catalytic activity of oxidized product shown in figure S5. The oxidized product turns into a colorless product with the passage of time while the IL due to its attractive properties not only stabilized the nanomaterial but also enhanced the long-term stability of TMB. It has been reported in the literature that instability is one of the alarming constituents of the catalyzed product whereas our work has demonstrated the long term stability. Up to the best of our knowledge, very rare data of long-time stability of the catalyzed product is available in literature and stability of catalyzed product can pursue

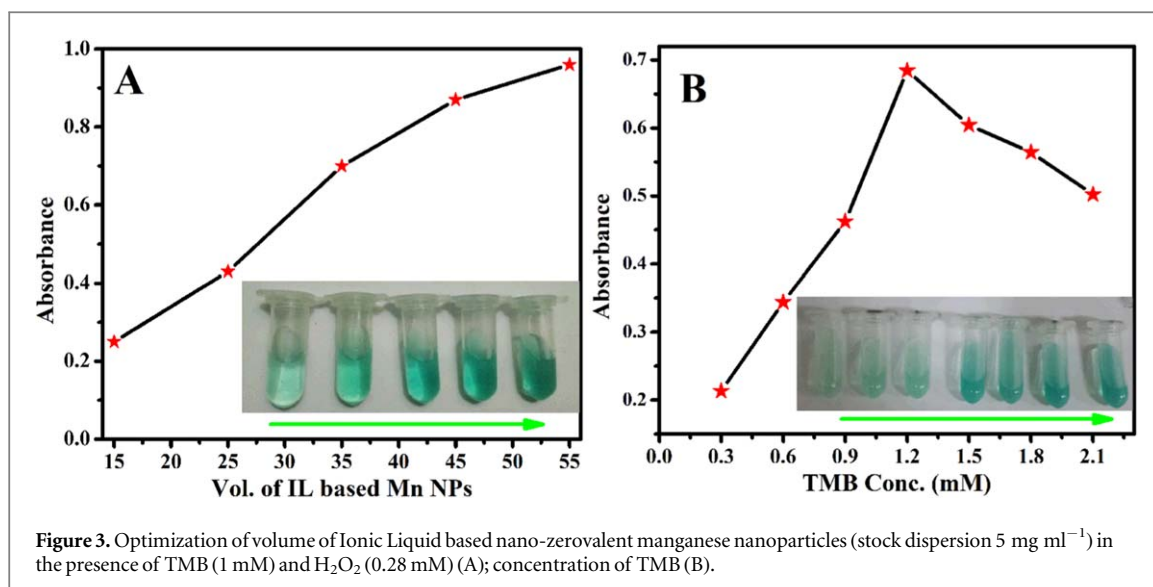


Figure 3. Optimization of volume of Ionic Liquid based nano-zerovalent manganese nanoparticles (stock dispersion 5 mg ml^{-1}) in the presence of TMB (1 mM) and H_2O_2 (0.28 mM) (A); concentration of TMB (B).

Table 1. A comparison of the K_m and V_m values for the pure and IL-based ZV-Mn NPs.

Catalyst	K_m [mM]		V_m [10^{-8} MS^{-1}]	
	TMB	H_2O_2	TMB	H_2O_2
IL coated ZV-Mn NPs	0.32	0.59	9.1	6.8
Pure ZV-Mn NPs	0.21	4.2	5.2	12

a vital role in biomedical research. It has been verified that IL is not only a powerful stabilizing agent but also modulate and increase the catalytic properties of manganese nanoparticles without disrupting the surface properties. Although various types of ILs have been reported in the literature but for the catalytic activity, specific kind of IL (1-H-3-methylimidazolium formate) must be used having the aromaticity in its structure.

3.3. Optimization of experimental conditions

Optimization of experimental conditions play a crucial rule in order to obtain the high catalytic activity of artificial enzymes depending upon various factors, amount of biomimetic materials, volume of IL in reaction mixture, concentration of TMB and H_2O_2 . The maximum peroxidase-like catalytic activity was obtained under following conditions; pH 7.4, 25°C , 5 min incubation time, $35 \mu\text{l}$ IL coated NPs, 10 mM TMB and $2.8 \text{ mM H}_2\text{O}_2$ as shown in figure 3 (A-B). Moreover, our system worked at various pH value of buffer medium and high temperature due to the good stability of IL, indicating the stable catalytic activity of ZV-Mn NPs and the obtained catalyzed products.

The kinetic parameters were measured for the catalytic oxidation of TMB in the presence of H_2O_2 to determine the peroxidase-like catalytic activity of nanomaterials by using Line weaver-Burk plots including Michaelis - Menton (K_m) and maximum initial velocity (V_m) by changing the concentration of TMB and H_2O_2 . The kinetic parameters measured for IL coated ZV-Mn NPs and pure ZV-Mn NPs data are presented in table 1. To perform the kinetic analysis, the concentration of one substrate was varied while the other was kept constant. The comparative study was performed to measure the kinetic parameters of both IL coated ZV-Mn NPs as well as the pure ZV-Mn NPs. The obtained kinetic parameters for IL coated ZV-Mn NPs was many folds better than the pure ZV-Mn NPs. The lower K_m value suggests that the lower concentration of oxidizing agent (H_2O_2) is required to achieve maximum catalytic response with IL based ZV-Mn NPs.

3.4. Detection of hydrogen peroxide

A simple calorimetry assay was used to detect hydrogen peroxide based on the optimized experimental condition and biomimetic IL coated ZV-Mn NPs. There was a color change in a calorimetric method and this method was used to determine the direct relationship between the concentrations of H_2O_2 and obtained absorbance at 652 nm for IL coated ZV-Mn NPs as shown in figure 4(A). The method enabled us to detect the H_2O_2 with a linear range of $10\text{--}280 \mu\text{M}$, the obtained limit of detection (LOD) was $0.20 \mu\text{M}$; calibration curve presented in figure 4(B), and the standard deviation was 5 to 6% as shown in table S1. There are various methods

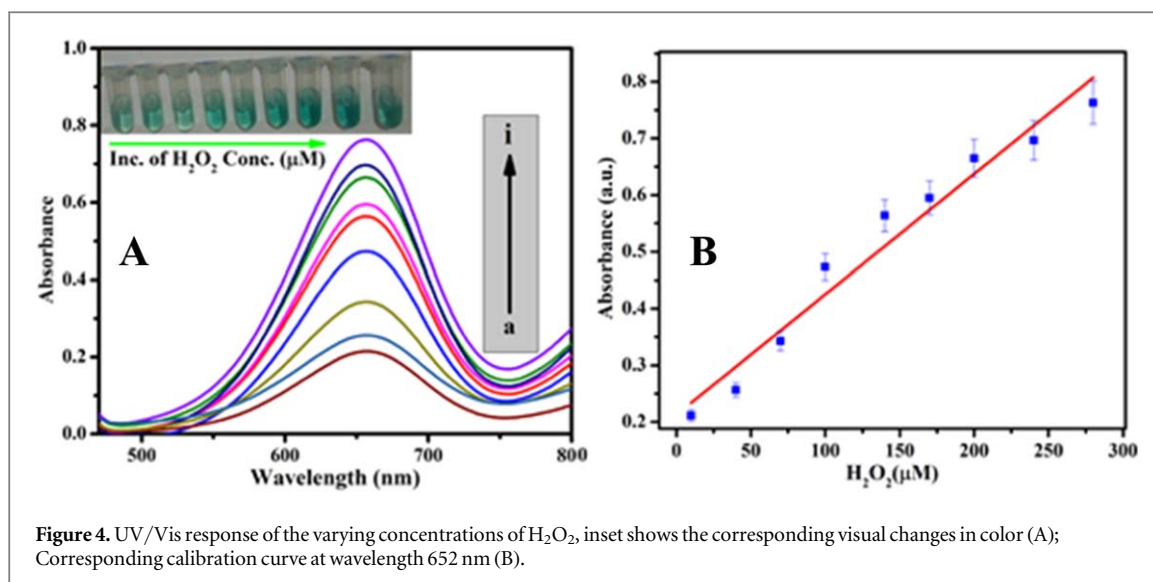


Figure 4. UV/Vis response of the varying concentrations of H₂O₂, inset shows the corresponding visual changes in color (A); Corresponding calibration curve at wavelength 652 nm (B).

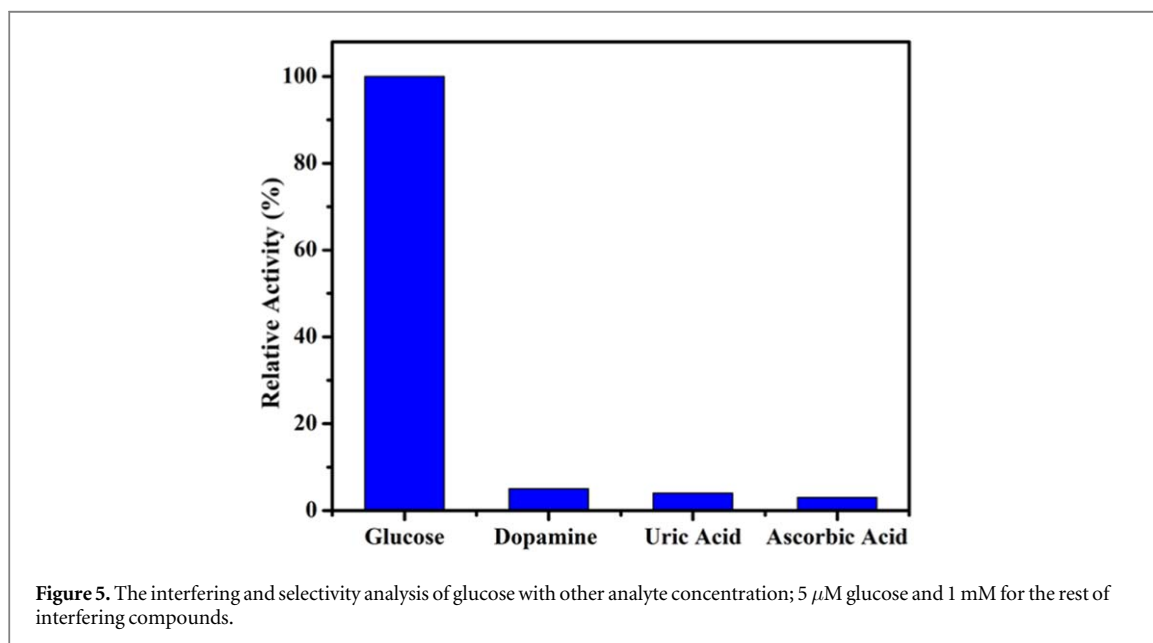


Figure 5. The interfering and selectivity analysis of glucose with other analyte concentration; 5 μM glucose and 1 mM for the rest of interfering compounds.

reported to detect H₂O₂ but the calorimetric method offers a very simple procedure and can be visualized with naked eyes. There is no need for any complex instruments or technical persons. In addition, the generation of OH radical as a result of adsorption of H₂O₂ on the nano-surface which are subsequently involved in the oxidation of TMB to give a blue-green color product.

3.5. Interference study

The selectivity of the proposed calorimetric detection based on the prepared IL coated ZV-Mn NPs as a peroxidase mimetic was further explored by studying the potential interfering compounds. The relative activity extracted from the investigating system of various interfering compounds such as dopamine, uric acid and ascorbic acid is shown in figure 5. From figure 5, it can be seen that the other interfering compounds having elevated concentration as compared to glucose showed very less response confirming the selectivity of the purposed peroxidase-like catalytic activity of IL coated ZV-Mn NPs induced by H₂O₂.

3.6. Real sample analysis

It is pretty known to everyone that H₂O₂ is used as stabilizer in commercial milk products but their residual must be controlled due to its harmful effects on the skin of human beings. The accredited maximum H₂O₂ quantity allowed by US FDA is 0.05 wt% (ca. 15 μM) [49]. Therefore, the sensitive and selective detection of H₂O₂ is mandatory for the long time storage of pasteurized milk used in practical and healthy life. In order to confirm the

Table 2. Colorimetric H₂O₂ sensor based on obtained recovery percentages.

Milk samples	Added (μM)	H ₂ O ₂ found (μM)	R.S.D % (μM)	R.E % (μM)	R % (μM)
1	250	247	3.2	3	98
2	180	171	3.8	4	96

real sample analysis, we have taken two samples of milk from Key Lab of Separation and Purification, Huazhang Agriculture Science University, Wuhan, China, the colorimetric detection of H₂O₂ was used under the optimized conditions to determine the concentration of H₂O₂ in two samples of acquired milk. Therefore, selective and sensitive detection of H₂O₂ is very important in the milk industry during the course of storing the pasteurized milk for long duration. Standard addition methods were used to detect H₂O₂ spiked in milk samples. Samples were tested two times, and then averaged H₂O₂ concentration was calculated from the calibration curve. The recoveries and relative standard deviation (RSD) values are acceptable for the proposed H₂O₂ sensor array as shown in table 2.

4. Conclusion

The present work demonstrated the peroxidase like catalytic activity of nano zerovalent manganese. In addition, the new type of IL namely 1 H-3-Methylimidazolium formate was utilized to modify the surface of ZV-Mn NPs to synergistically enhances its catalytic performance in oxidation of TMB by H₂O₂. The impact of work is associated with demonstration of ZV-Mn NPs as a peroxidase mimetic and application of IL coated ZV-Mn NPs for fast, highly sensitive and selective colorimetric detection of H₂O₂. The easy to prepare peroxidase mimetic, low degradation oxidized product, stable, and environmentally friendly procedure were investigated. This concept can be further extended to modulate the properties of nanozymes towards construction of colorimetric assays.

Acknowledgments

Sajid Rauf thanks the financial support from the Natural Science Foundation of China (No. 11674086) and Hubei Provincial Department of Education (D20181004).

Compliance with ethical standards

The author(s) declare that they have no competing interests.

Conflict of interest

The author(s) declares no conflict of interest.

ORCID iDs

Sajid Rauf  <https://orcid.org/0000-0003-2343-9334>

Nasir Ali  <https://orcid.org/0000-0001-5028-4265>

MAK Yousaf Shah  <https://orcid.org/0000-0002-1081-9090>

References

- [1] Wang N *et al* 2015 A Cu₂(OH)₃Cl-CeO₂ nanocomposite with peroxidase-like activity, and its application to the determination of hydrogen peroxide, glucose and cholesterol *Microchim. Acta* **182** 1733–8
- [2] Kirkman H N and Gaetani G F 2007 Mammalian catalase: a venerable enzyme with new mysteries *Trends Biochem. Sci* **32** 44–50
- [3] Pierre A 2004 The sol-gel encapsulation of enzymes *Biocatal. Biotransform.* **22** 145–70
- [4] Salimi A *et al* 2007 Nanomolar detection of hydrogen peroxide on glassy carbon electrode modified with electrodeposited cobalt oxide nanoparticles *Anal. Chim. Acta* **594** 24–31
- [5] Lu W *et al* 2011 Synthesis of functional SiO₂-coated graphene oxide nanosheets decorated with Ag nanoparticles for H₂O₂ and glucose detection *Biosens. Bioelectron.* **26** 4791–7
- [6] Li Q *et al* 2012 One-pot synthesis of Ag nanoparticles/reduced graphene oxide nanocomposites and their application for nonenzymatic H₂O₂ detection *Electrochim. Acta* **83** 283–7

- [7] Chang G *et al* 2012 Ag nanoparticles decorated polyaniline nanofibers: synthesis, characterization, and applications toward catalytic reduction of 4-nitrophenol and electrochemical detection of H₂O₂ and glucose *Catalysis Science & Technology* **2** 800–6
- [8] Zhou D *et al* 2017 Fe₃N-Co₂N nanowires array: a non-noble-metal bifunctional catalyst electrode for high-performance glucose oxidation and H₂O₂ reduction toward non-enzymatic sensing applications. *Chemistry-A European Journal* **23** 5214–8
- [9] Wang Z *et al* 2017 Copper-nitride nanowires array: an efficient dual-functional catalyst electrode for sensitive and selective non-enzymatic glucose and hydrogen peroxide sensing. *Chemistry-A European Journal* **23** 4986–9
- [10] Xie F *et al* 2018 Cobalt nitride nanowire array as an efficient electrochemical sensor for glucose and H₂O₂ detection *Sensors Actuators B* **255** 1254–61
- [11] Xiong X *et al* 2017 Ni₂P nanosheets array as a novel electrochemical catalyst electrode for non-enzymatic H₂O₂ sensing *Electrochim. Acta* **253** 517–21
- [12] Wang Z *et al* 2017 High-performance non-enzyme hydrogen peroxide detection in neutral solution: using a nickel borate nanoarray as a 3D electrochemical sensor. *Chemistry-A European Journal* **23** 16179–83
- [13] Tian J *et al* 2013 Ultrathin graphitic carbon nitride nanosheets: a low-cost, green, and highly efficient electrocatalyst toward the reduction of hydrogen peroxide and its glucose biosensing application *Nanoscale* **5** 8921–4
- [14] Nasir M *et al* 2017 An overview on enzyme-mimicking nanomaterials for use in electrochemical and optical assays *Microchim. Acta* **184** 323–42
- [15] Hurdis E and Romeyn H 1954 Accuracy of determination of hydrogen peroxide by cerate oxidimetry *Anal. Chem.* **26** 320–5
- [16] Wang L *et al* 2014 AgNP-DNA@GQDs hybrid: new approach for sensitive detection of H₂O₂ and glucose via simultaneous AgNP etching and DNA cleavage *Anal. Chem.* **86** 12348–54
- [17] Hu Y *et al* 2019 Determination of the activity of alkaline phosphatase based on aggregation-induced quenching of the fluorescence of copper nanoclusters *Microchim. Acta* **186** 5
- [18] Liu S *et al* 2012 A general strategy for the production of photoluminescent carbon nitride dots from organic amines and their application as novel peroxidase-like catalysts for colorimetric detection of H₂O₂ and glucose *RSC Adv.* **2** 411–3
- [19] Chen S *et al* 2014 In situ growth of silver nanoparticles on graphene quantum dots for ultrasensitive colorimetric detection of H₂O₂ and glucose *Anal. Chem.* **86** 6689–94
- [20] Tian J *et al* 2013 Ultrathin graphitic carbon nitride nanosheets: a novel peroxidase mimetic, Fe doping-mediated catalytic performance enhancement and application to rapid, highly sensitive optical detection of glucose *Nanoscale* **5** 11604–9
- [21] Zhang R *et al* 2020 Ultrasensitive aptamer-based protein assays based on one-dimensional core-shell nanozymes *Biosens. Bioelectron.* **150** 111881
- [22] Zhou Y *et al* 2019 Enhanced synergistic effects from multiple iron oxide nanoparticles encapsulated within nitrogen-doped carbon nanocages for simple and label-free visual detection of blood glucose *Nanotechnology* **30** 355501
- [23] Zheng J *et al* 2019 Enhanced peroxidase-like activity of hierarchical MoS₂-decorated N-doped carbon nanotubes with synergetic effect for colorimetric detection of H₂O₂ and ascorbic acid *Chin. Chem. Lett.* (<https://doi.org/10.1016/j.ccl.2019.09.037>)
- [24] Cao T *et al* 2019 Increasing enzyme-like activity by in situ anchoring of Ag₃PO₄ nanoparticles on keratin-inorganic hybrid nanoflowers *New J. Chem.* **43** 15946–55
- [25] Wu N *et al* 2019 Enhanced peroxidase-like activity of AuNPs loaded graphitic carbon nitride nanosheets for colorimetric biosensing *Anal. Chim. Acta* **1091** 69–75
- [26] Dehghani Z, Mohammadnejad J and Hosseini M 2019 A new colorimetric assay for amylase based on starch-supported Cu/Au nanocluster peroxidase-like activity *Anal. Bioanal. Chem.* **411** 3621–9
- [27] Breslow R 1995 Biomimetic chemistry and artificial enzymes: catalysis by design *Acc. Chem. Res.* **28** 146–53
- [28] Wei H and Wang E 2013 Nanomaterials with enzyme-like characteristics (nanozymes): next-generation artificial enzymes *Chem. Soc. Rev.* **42** 6060–93
- [29] Nasir M *et al* 2017 Biomimetic nitrogen doped titania nanoparticles as a colorimetric platform for hydrogen peroxide detection *J. Colloid Interface Sci.* **505** 1147–57
- [30] Jiang H *et al* 2012 Peroxidase-like activity of chitosan stabilized silver nanoparticles for visual and colorimetric detection of glucose *Analyst* **137** 5560–4
- [31] André R *et al* 2011 V₂O₅ nanowires with an intrinsic peroxidase-like activity. *Adv. Funct. Mater.* **21** 501–9
- [32] Cui R, Han Z and Zhu JJ 2011 Helical carbon nanotubes: intrinsic peroxidase catalytic activity and its application for biocatalysis and biosensing *Chemistry-A European Journal* **17** 9377–84
- [33] Song Y *et al* 2010 Graphene oxide: intrinsic peroxidase catalytic activity and its application to glucose detection *Adv. Mater.* **22** 2206–10
- [34] Rauf S *et al* 2017 Protic ionic liquids as a versatile modulator and stabilizer in regulating artificial peroxidase activity of carbon materials for glucose colorimetric sensing *J. Mol. Liq.* **243** 333–40
- [35] van Rantwijk F, Lau R M and Sheldon R A 2003 Biocatalytic transformations in ionic liquids *Trends Biotechnol.* **21** 131–8
- [36] Cull S *et al* 2000 Room-temperature ionic liquids as replacements for organic solvents in multiphase bioprocess operations. *Biotechnol. Bioeng.* **69** 227–33
- [37] Liu J-f, Jiang G-b and Jönsson J Å 2005 Application of ionic liquids in analytical chemistry *TrAC, Trends Anal. Chem.* **24** 20–7
- [38] Lee J W *et al* 2010 Toward understanding the origin of positive effects of ionic liquids on catalysis: formation of more reactive catalysts and stabilization of reactive intermediates and transition states in ionic liquids *Acc. Chem. Res.* **43** 985–94
- [39] Lin Y *et al* 2013 Ionic liquid as an efficient modulator on artificial enzyme system: toward the realization of high-temperature catalytic reactions *J. Am. Chem. Soc.* **135** 4207–10
- [40] Qian W *et al* 2012 Properties of pure 1-methylimidazolium acetate ionic liquid and its binary mixtures with alcohols *The Journal of Chemical Thermodynamics* **49** 87–94
- [41] Wan Z and Wang J 2017 Degradation of sulfamethazine antibiotics using Fe₃O₄-Mn₃O₄ nanocomposite as a Fenton-like catalyst *Journal of Chemical Technology & Biotechnology* **92** 874–83
- [42] Soboleva T *et al* 2010 On the Micro-, Meso-, and macroporous structures of polymer electrolyte membrane fuel cell catalyst layers *ACS Applied Materials & Interfaces* **2** 375–84
- [43] Kruk M and Jaroniec M 2001 Gas Adsorption Characterization of Ordered Organic-Inorganic Nanocomposite Materials *Chem. Mater.* **13** 3169–83
- [44] Zhang G-S *et al* 2007 Removal mechanism of as(III) by a novel Fe-Mn binary oxide adsorbent: oxidation and sorption *Environmental Science & Technology* **41** 4613–9
- [45] Peng B *et al* 2016 Facile synthesis of Fe₃O₄@Cu(OH)₂ composites and their arsenic adsorption application *Chem. Eng. J.* **299** 15–22
- [46] Panda A P *et al* 2019 Core-shell structured zero-valent manganese (ZVM): a novel nanoadsorbent for efficient removal of as(iii) and As(v) from drinking water *Journal of Materials Chemistry A* **7** 9933–47

- [47] Wang Y, Zhao H and Zhao G 2015 Iron-copper bimetallic nanoparticles embedded within ordered mesoporous carbon as effective and stable heterogeneous Fenton catalyst for the degradation of organic contaminants *Appl. Catalysis B* **164** 396–406
- [48] Zarif F *et al* 2018 Ionic liquid coated iron nanoparticles are promising peroxidase mimics for optical determination of H₂O₂ *Microchim. Acta* **185** 302
- [49] Lu C-P *et al* 2011 Nitrophenylboronic acids as highly chemoselective probes to detect hydrogen peroxide in foods and agricultural products *J. Agric. Food Chem.* **59** 11403–6